Aquaculture 582 (2024) 740496

Contents lists available at ScienceDirect

Aquaculture

journal homepage: www.elsevier.com/locate/aquaculture

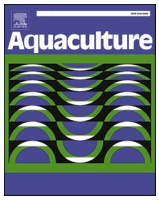

Knockout of Hermansky-Pudlak syndrome 5 (*hps5*) leads to red tilapia with reduced melanophores and iridophores

Chenxu Wang [a], Thomas D. Kocher [b], Hao Liu [a], Zilong Wen [a], Jiawen Yao [a], Deshou Wang [a,*]

[a] Integrative Science Center of Germplasm Creation in Western China (CHONGQING) Science City, Key Laboratory of Freshwater Fish Reproduction and Development (Ministry of Education), Key Laboratory of Aquatic Science of Chongqing, School of Life Sciences, Southwest University, Chongqing 400715, China
[b] Department of Biology, University of Maryland College Park, MD 20742, USA

ARTICLE INFO

Keywords:
hps5 mutation
Melanophores and iridophores
Xanthophores
Red body color
tilapia

ABSTRACT

Tilapia as an economically important fish is also an excellent model for studying pigment cell biology and body color formation. In the present study, we engineered a red tilapia by mutation of *hps5* using CRISPR/Cas9 gene editing of a target site in exon 2. Disruption of HPS5 led to a significant decrease in the numbers of melanophores and iridophores, and a significant increase in xanthophores, which led to a yellowish-transparent body color in early stages (5–30 dpf, days post fertilization). Slow recovery of iridophore numbers, and increased numbers of xanthophores with shorter nearest-neighbor distances than in wild-type fish was observed at 150 dpf, which finally led to a red tilapia with reddish pigmentation in fins. The *hps5*$^{-/-}$ mutants also showed several transparent cracks (absence of melanin, iridophores and xanthophores) in iris development. Besides, *hps5* was also found to be fundamental for xanthophore development, and even the distance between each of them. Our *hps5* mutants provide an excellent new model for studies of HPS5 function. Additionally, the red tilapia mutants may also have potential to serve as new germplasm for aquaculture, or function as a gene resource for genetic modification and breeding of red tilapia and the other related ornamental and food fish in aquaculture. More importantly, this study may have significant values in the area of development and evolution of pigmentation patterns of fish species.

1. Introduction

Melanophores are the most common pigment cell in vertebrates, and during the past 250 years, many studies of pigment-disordered diseases (e.g. albinism, vitiligo and melanoma) were focused on this type of pigment cell. So far, >200 genes have been associated with melanosome biosynthesis and melanophore differentiation in human and mouse, among which the tyrosinase family members (including *tyr*, *tyrp1* and *tyrp2/dct*) are the most widely studied in vertebrate species. For melanin synthesis to occur, melanogenic enzymes must be trafficked from the Golgi to the developing melanosome. The BLOC (biogenesis of lysosome-related organelles complex) super family, including BLOC1-BLOC3, is fundamental for this process in mouse and human beings (Wei, 2006; Sitaram and Marks, 2012). BLOC1 family is composed of *dysbindin* (*dtnbp1/hps7*), *bloc1s1-bloc1s3* (*blos1-blos3/hps8*), *pallidin* (*pldn/hps9*), *cappuccino/cno*, *snapin* and *muted*; BLOC2 family is composed of *hps3*, *hps5* and *hps6*, and BLOC3 family is composed of *hps1* and *hps4*. *Hps3*, *hps5* and *hps6* are known to function together as the Bloc2 complex to influence tyrosinase trafficking and melanosome biosynthesis (Wei, 2006; Daly et al., 2013). *Hps5* mutation has been found to be closely linked with the pink eye phenotype in *Drosophila* (Falcón-Pérez et al., 2007; Syrzycka et al., 2007), the translucent phenotype in the silkworm larvae (Fujii et al., 2012), eumelanin and pheomelanin biosynthesis in mouse (Hirobe et al., 2013), *snow white* phenotype in zebrafish (Daly et al., 2013), *casper* phenotype in stickleback (Hart and Miller, 2017), and ocular albinism in donskoy cats (Mériot et al., 2020). All these phenotypes are closely related to melanogenesis, a process which is highly conserved in teleosts and other animals (Braasch et al., 2009; Bian et al., 2021).

Pigment cells including melanophores, xanthophores and

Abbreviations: CRISPR/Cas9, clustered regularly interspaced short palindromic repeats/CRISPR associated protein 9; HPS5, Hermansky-Pudlak syndrome 5 protein; RPE, retinal pigment epithelium; LROs, lysosome-related organelles; BLOC1, biogenesis of lysosome-related organelles complex 1; BLOC2, biogenesis of lysosome-related organelles complex 2; BLOC3, biogenesis of lysosome-related organelles complex 3..

* Corresponding author.
E-mail address: wdeshou@swu.edu.cn (D. Wang).

https://doi.org/10.1016/j.aquaculture.2023.740496
Received 17 October 2023; Received in revised form 25 November 2023; Accepted 17 December 2023
Available online 19 December 2023

iridophores are the foundation of body color in most teleosts. Besides the decrease of melanophores and melanosomes, mutation of *hps5* also led to significant decrease of iridophores in stickleback (Hart and Miller, 2017) and the absence of iridophores in zebrafish (Daly et al., 2013). It is unclear whether the differences in iridophore phenotype are due to species differences or to recovery of iridophores during later development, as the phenotype was observed at adult stage in stickleback and at larval stage in zebrafish. Furthermore, in tilapia mutation of melanogenesis-related genes usually results in changes of pigment cell relative abundance and pigment cell size (Wang et al., 2022a; Lu et al., 2022; Wang et al., 2022b; Wang et al., 2023). It would be interesting to know whether mutation of *hps5* influences the number and size of other types of pigment cells, especially the xanthophores and erythrophores.

We have successfully mutated dozens of the color genes and developed the Nile tilapia as a model for studying teleost color patterning (Wang et al., 2021). Mutation of *hps4* results in an albino phenotype with complete loss of melanophore pigmentation, generating a silver-white tilapia (Wang et al., 2022b). In this study, we disrupted *hps5* using CRISPR/Cas9 and characterized the coloration phenotypes at various developmental stages. Strikingly, in addition to affecting melanophore and iridophore survival and pigmentation, mutation of *hps5* also altered the number and size of xanthophores in tilapia. Adult fish showed a red body color. Interestingly, the *hps5*$^{-/-}$ mutants displayed several transparent cracks (lack of melanin, iridophore and xanthophore pigmentation, thus allowing visualization of the RPE coloration) in the iris from ~90 dpf onwards. Our study provides valuable information toward understanding the roles of *hps5* in pigment cell biology in teleosts, and the red mutants provide new germplasm for developing aquaculture strains.

2. Materials and methods

2.1. Fish

The founder strain of Nile tilapia was a gift from Prof. Nagahama (Laboratory of Reproductive Biology, National Institute for Basic Biology, Okazaki, Japan). This strain has been domesticated for over 20 years and is therefore highly homozygous. Experimental fish were reared in recirculating aerated freshwater tanks and maintained at room temperature (27 °C) under a natural photoperiod. Before each experiment the fish were kept under 15:9 h light: dark conditions at 27 ± 1 °C for 7 days. All animal experiments followed the regulations of the Guide for the Care and Use of Laboratory Animals and were approved by the Committee for Laboratory Animal Experimentation of Southwest University.

2.2. The expression pattern analysis of hps5 in different tissues

The expression patterns of *hps5* in different tissues of Nile tilapia were downloaded from NCBI database (Brawand et al., 2014). To validate these expression levels we designed *hps5* specific primers for reverse transcription PCR amplification using Primer Premier 6. The F/R sequences (*hps5*-RT-F/R) are listed in Table S1. Triplicate samples of 15 different tissues were collected at the adult stage. Reverse transcription was conducted in a total reaction volume of 20 μl, which included 2 μg total RNA and 2 μl RT reaction mixture. For PCR amplification, *hps5* specific primers or *β*-actin primers were added to the reaction at the beginning of PCR and each PCR run for 34 cycles. The PCR products were separated by agarose gel electrophoresis and photographed under UV illumination, as described in our previous study (Wang et al., 2022b).

2.3. Establishment of hps5$^{-/-}$ mutants by CRISPR/Cas9

CRISPR/Cas9 editing was used to knockout *hps5* in tilapia as described previously (Wang et al., 2021). Briefly, the guide RNA and Cas9 mRNA were co-injected into one-cell-stage embryos at a concentration of 150 and 500 ng/μL, respectively. About 400 fertilized eggs were used for target gene editing and 100 for control. Twenty injected embryos were randomly collected 72 h after injection. Genomic DNA was extracted from the pooled control and injected embryos and used to characterize the mutations. DNA fragments covering the target site were amplified. The gene-specific sequences are listed in Table S1. The mutated sequences were analyzed by restriction enzyme digestion with *Hpy*188I and Sanger sequencing.

The *hps5* mutants with the highest indel frequency were selected as F0 founders. Heterozygous F1 offspring were obtained by crossing F0 XY male founders to WT XX females. F1 larval fish were collected at 10 dah (days after hatching) and genotyped by PCR amplification and subsequent enzyme digestion. The F1 fish were genotyped by fin clip assay and the individuals with frame-shift mutations were selected. XY male and XX female siblings of the F1 generation, carrying the same type of mutation, were mated to generate the homozygous F2 mutants. The *hps5*$^{-/-}$ mutants were screened from the F2 offspring using restriction enzyme digestion and Sanger sequencing. The genetic sex of every fish was determined by genotyping using a sex-linked marker (Marker 5) described previously (Sun et al., 2014).

2.4. Image recording and pigment cell analysis of the mutants and wild-type fish

Larval fish at 12 dpf and 30 dpf were first anesthetized with tricaine methasulfonate (MS-222, Sigma-Aldrich, USA), then shifted to an observation dish with clean water, photographed from the lateral view by Olympus SZX16 stereomicroscope (Olympus, Japan) under bright field and transparent field with various magnification. The 90 and 150 dpf wild-type and mutant fish were shifted to 30 × 5 × 20 cm^3 glass water tanks and photographed with a Nikon D7000 digital camera (Nikon, Japan) against a blue background. The caudal fins of fish at 150 dpf were removed with medical scissors, soaked in 0.65% Ringers' solution and directly observed with Olympus SZX16 stereomicroscope without cover slip under transparent or bright field. Scales of fish at 150 dpf were soaked in 0.65% Ringers' solution under cover slip, and were observed under Leica EM UC7 microscope (Leica, Germany). To analyze the number of pigment cells, 5 mutants and 5 wild-type fish were anesthetized with tricaine methasulfonate (MS-222, Sigma-Aldrich, USA) and immersed in 10 mg/ml epinephrine (Sigma, USA) solution for 15 min to contract pigment granules. Image recording of pigment cells was conducted as quickly as possible after putting them in the Ringers' solution as the preparations were not stable. The sizes of xanthophores, relative iridophore and melanin content, and distances between xanthophores were measured using Image J software (Schneider et al., 2012). For more detaily, the relative abundance of melanin and iridophores were measured by the dividing the melanin pigmentation area and iridescent area by the iris area (the entire circular area), respectively. ACDSee Official Edition software (ACDSystems, Canada) and Adobe Illustrator CS6 (Adobe Inc. USA) were used to format the pictures.

2.5. Melanin quantification

To analyze the number of melanophores, three fish per group were anesthetized with tricaine methasulfonate (MS-222, Sigma-Aldrich, USA). Skin sample suspensions were solubilized in 8 M urea/1 M sodium hydroxide and cleared by centrifugation at 10,700*g* for 10 min. Chloroform was added to the supernatants to remove fatty impurities. Skin samples were cleared by centrifugation at 10,700*g* for 10 min and analyzed for absorbance at 400 nm, as we showed in our previous studies (Wang et al., 2022b).

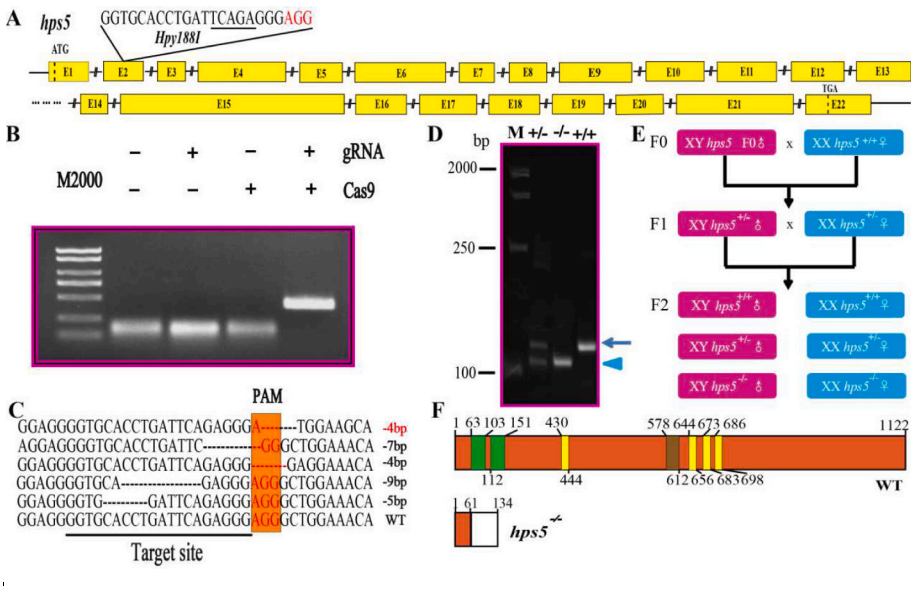

Fig. 1. Establishment of *hps5*$^{-/-}$ (A-F) mutant line in Nile tilapia.
A: Gene structures of *hps5* showing the target site and the *Hpy*188I restriction site. B: Restriction enzyme digestion of the amplified fragment of *hps5* using primers spanning the target sites. The Cas9 mRNA and gRNA were added as indicated. C: Sanger sequencing results from the uncleaved bands were listed. The PAM is marked in orange. Deletions are marked by dashes (−) and numbers to the right of the sequences indicate the loss of bases for each allele. WT, wild type. D: Identification of *hps5* F2 genotypes by hetero-duplex motility assay. Arrowheads show homo-duplexes and arrows show hetero-duplexes. E: Schematic diagram showing the breeding plans of *hps5* F0 to F2 fish. F: Tilapia HPS5 intact (with two WD40 domains, green boxes; four low complexity regions, golden boxes; and one coiled coil region, brown box) and mutated protein. Mutation of *hps5* resulted in a truncated protein composed of 134 amino acids. (For interpretation of the references to color in this figure legend, the reader is referred to the web version of this article.)

2.6. Modeling and image processing

Shapr 3D software (Shapr 3D systems, Hungary), ACDSee Official Edition software (ACDSystems, Canada), Adobe Illustrator CS6 (Adobe Inc. USA) and Image J software (Schneider et al., 2012) were used to format the pictures and modeling of global body color, eye color patterning, pigment cell development and pigment cell relative abundance of the wild-type fish and the color mutants.

2.7. Data analysis

Data are expressed as mean ± SD. GraphPad Prism 5.01 software (Graphpad, USA) was used to analyze and export the differences in the number and sizes of pigment cells, xanthophore distances and melanin contents in *hps5*$^{-/-}$ mutants and wild type fish. Differences in the data between wild-type and mutants were tested by a two-tailed Student's *t*-test (***, $P < 0.001$; **, $P < 0.01$; *, $P < 0.05$; ns, not significant).

3. Results

3.1. Gene structure and functional domains of hps5/HPS5 in Nile tilapia

The Nile tilapia *hps5* gene has 22 exons (Fig. 1A). Functional domain prediction by SMART showed two WD40 domains (Fig. 1F, indicated by green boxes), four low complexity regions (Fig. 1F, indicated golden boxes) and one coiled coil region (Fig. 1F, indicated by brown box) in the amino acid sequence of HPS5. Like *hps* family members in human and mouse (Wei, 2006), *hps5* was ubiquitously expressed in many tissues of tilapia, but most highly expressed in ovary, eyes and kidney (Fig. S1).

3.2. Establishment of the hps5$^{-/-}$ mutant line in tilapia

To disrupt tilapia *hps5* we targeted a site in exon 2 with CRISPR-cas9. The sequence of gRNA target was GGTGCACCTGATTCAGAGGGAGG, in which AGG was the PAM region (Fig. 1A and C). F0 founders were screened by restriction enzyme digestion with *Hpy*188I and Sanger sequencing (Fig. 1B and C). In the *hps5* F0 chimeras, significant hypopigmentation was observed in the head and body, and part of the trunk surface were complete white and even partially transparent (Fig. S2). The results suggest that *hps5* is fundamental for body color formation in tilapia. The *hps5* mutant fish (XY male) with a high mutation rate (over 75%) were raised to sexual maturity and mated with wild-type tilapia (XX femaile) to create F1 fish. Heterozygous *hps5* F1 offspring with a − 4 bp deletion in the second exon were selected to breed the F2 generation. As a result, a truncated protein of only 134 amino acids were produced in the homozygous mutants (Fig. 1D and E).

3.3. Melanophores and iridophores were significantly reduced in the mutants from early embryonic stages

Just as predicted, there were significant differences of pigment cell numbers between the wild-type fish and the *hps5*$^{-/-}$ mutants from very early embryonic stages. In the wild-type embryos melanophores were detected in an increasing wave at 3 dpf, and many branching-like mature melanophores were detected on the yolk sac. Many melanophores and iridophores were detected in the iris, and the RPE was detected with many melanosomes (Fig. 2A). Many melanophores and iridophores were detected in the iris, and many mature melanophores were also detected on the yolk sac at 4 dpf. Pigment cells were not uniformly distributed in the iris, thus a black crack-like pattern (without melanophores or iridophores) was detected in the iris (Fig. 2B). At 5 dpf many melanophores were detected on the yolk sac and the top of the head. The iris had increasing numbers of iridophores, but no black crack-like pattern was detected (Fig. 2C). At 7 dpf, a second increase of melanophores was detected on the top of the head and the peritoneum. A large increase in iridophores was detected on the peritoneum and iris of wild-type embryos (Fig. 2D). At 8 dpf many melanophores were detected on top of the head, trunk, peritoneum and yolk sac. Many iridophores were also detected in the peritoneum and iris at this time. The whole eyes (including RPE and iris) were populated with melanosomes, under

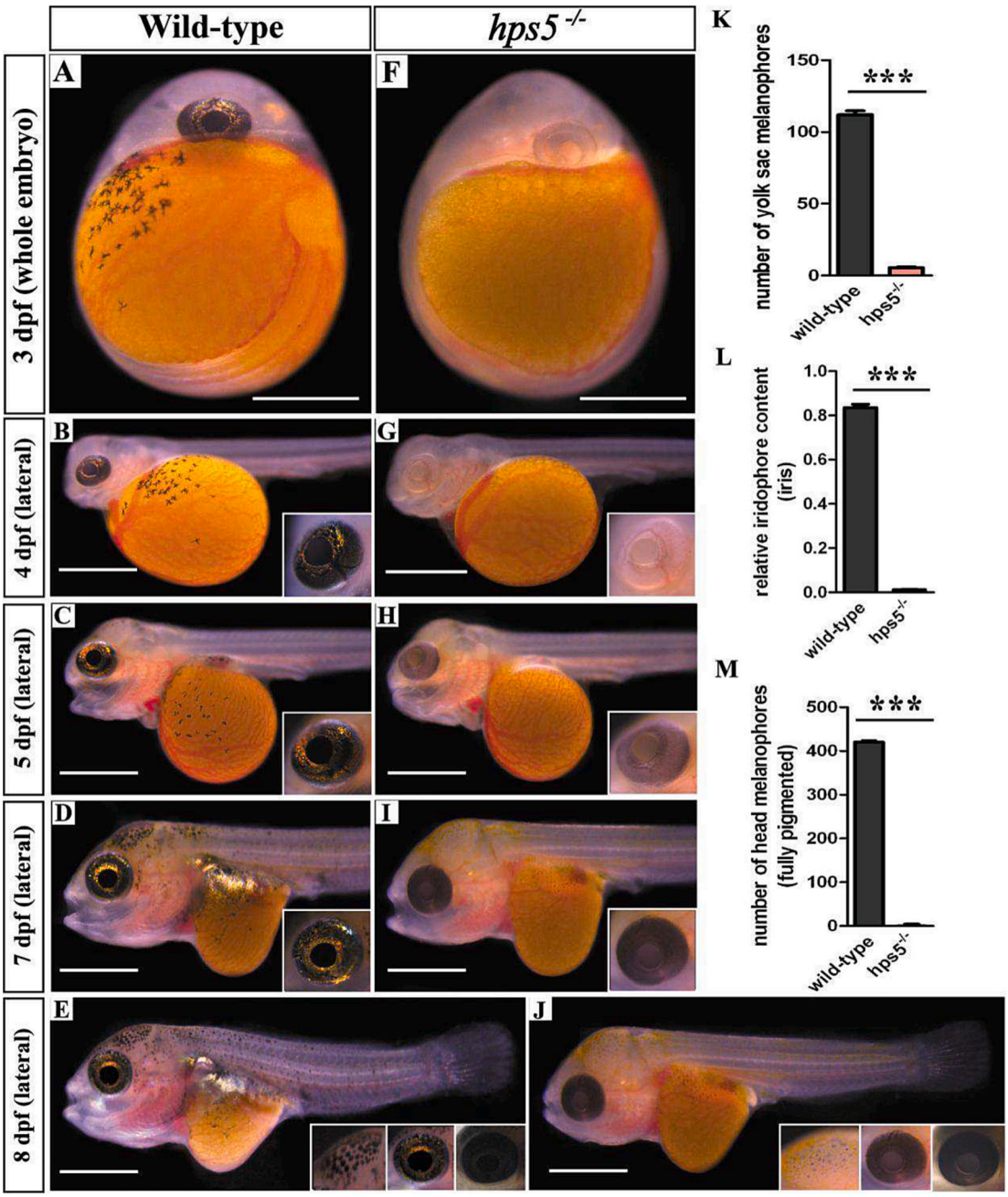

Fig. 2. Significantly reduced melanophores and iridophores were detected in the mutants than in wild-type embryos.
A-E: Wild-type embryos. Many clustered and fully pigmented melanophores were detected in the yolk sac, and many melanophores and iridophores were detected in the iris of the wild-type embryos at 3 dpf (A). Many melanophores were detected in the yolk sac and many iridophores and xanthophores were also detected in the iris of the embryos at 4 dpf (B). Many melanophores were gathering toward the gill and heart in the yolk sac, and some melanophores were also observed in the top head. Many melanophores and inceasing amounts of iridophores were detected in the iris (C). Vast accumulation of the melanophores were observed in the top head, and many melanophores and iridophores were observed in the peritoneum. Additionally, the RPE was in black coloration, same to the results in 3–5 dpf embryos. The iris was detected with many iridophores and melanophores (D). Similar to the results in 7 dpf embryos, many melanophores on the top head and fully pigmented iris, RPE and peritoneum were detected in the 8 dpf embryos. F-J: The *hps5*$^{-/-}$ mutant embryos. No pigmented melanophores nor melanosomes were detected in the yolk sac or eyes (RPE and iris) of the 3 dpf mutants (F). Similar situation was detected in the whole embryos of the 4 dpf mutants. While it should be not ignored that the iris was detected with an obvious capillary network patches (G). Surprisingly, the mutant embryos were detected with few hypo-pigmented melanophores in the yolk sac and the top head, and the RPE and iris were detected with a slow restoration of melanosomes and melanophores. Additionally, a vast accumulation of xanthophores were detected in the top head at 5 dpf (H). Increasing xanthophores were detected in the head and the trunk, melanophores and melanosomes kept increasing in the iris and the RPE, respectively, while the RPE was still hypo-pigmented compared with the wild-type embryos at 7 dpf. Few hypo-pigmented melanophores were detected in the yolk sack but some hypo-pigmented melanophores were detected in the top head. The peritoneum showed a transparent color due to loss of melanophores and iridophores (I). An ovbious accumulation of large-sized xanthophores and many hypo-pigmented melanophores were detected in the top head of the 8 dpf mutants. The whole eyes were detected with increasing black pigmentation compared with the earlier mutant embryos, but still in hypo-pigmentation compared with the wild-type eyes. The peritoneum was transparent and increasing xanthophores were observed in the trunk (J). K-M: Quantification of the number of the yolk sac melanophores at 3 dpf, relative iridophore content in iris at 5 dpf, and number of the head melanophores at 8 dpf in the mutant and the wild-type embryos. Data in K-M are expressed as mean ± SD ($n = 5$). Differences in the data between wild-type and mutant embryos were tested by two-tailed Student's *t*-test, $^{***}P < 0.001$.

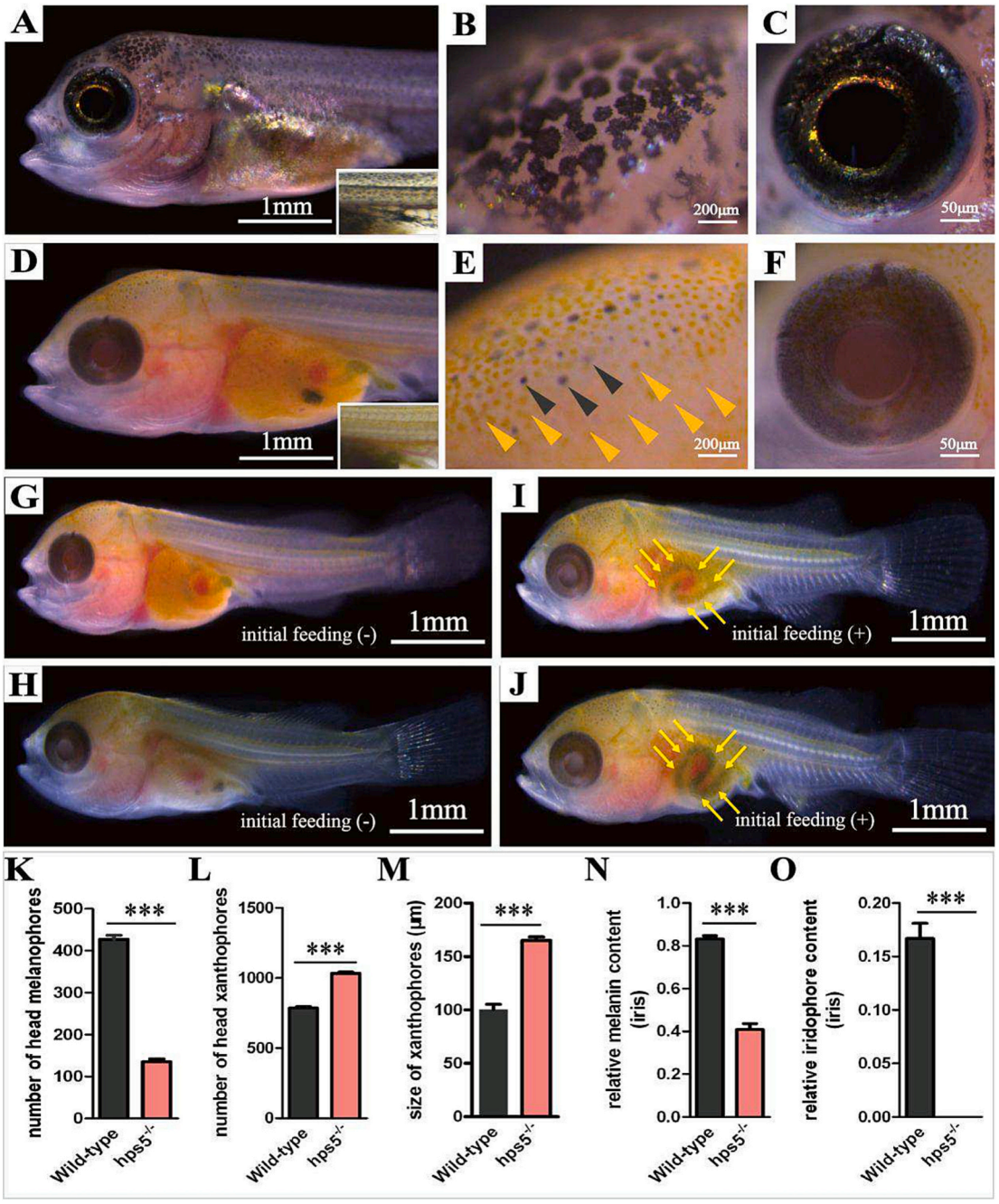

Fig. 3. Melanophores were hypo-pigmented and significantly decreased, iridophores were absent, while xanthophores were significant increased in number and sizes in head of the mutants at 12 dpf.

A-C: Wild-type fish. Many evenly distributed melanophores were detected in the trunk and iris. The RPE was black, and the iris was detected with many melanophores and iridophores (A). Higher magnification of the top head showing the macro-melanophores and iridophores (B). Dark melanin was observed in the RPE, and many melanophores and iridophores were observed in the iris (C). D-F: *hps5*$^{-/-}$ mutants. Complete transparent body color was detected, with a few hypo-pigmented melanophores, but no iridophores in the head and absence of iridophores in the trunk, iris and fins. In contrast, significantly increased xanthophores with significant larger sizes were observed in the whole fish (D). Higher magnification of the top head showing significant reduced and hypo-pigmented melanophores (black arrow heads) with immature melanosmes and significantly increased and larger sized xanthophores (yellow arrow heads) (E). The RPE was hypo-pigmented and showed a dark red coloration, but still with some melanin. The iris was detected with a few melanosomes, but the content was sinigicant lower than in wild-type fish. No iridophores were observed in the iris (F). G, H: The mutants were detected with a global transparent body color in whole trunk and fins, and the peritoneum was also highly transparent, revealed by the color and location of the inner organs like the liver, gut, etc. I, J: Strikingly, the 12 dpf mutants were detected with the most accurate location and morphology of the intestines after taking the initial feeding. K, N and O: Quantitative analysis of the numbers of the melanophores, relative melanin and iridophore content in the head and eyes of the mutants and wild-type fish. L, M: Quantitative analysis of the xanthophore numbers and sizes in the top head. Data in K—O are expressed as mean ± SD (n = 5). Differences in the data between wild-type and mutants were tested by two-tailed Student's *t*-test, ***P < 0.001. (For interpretation of the references to color in this figure legend, the reader is referred to the web version of this article.)

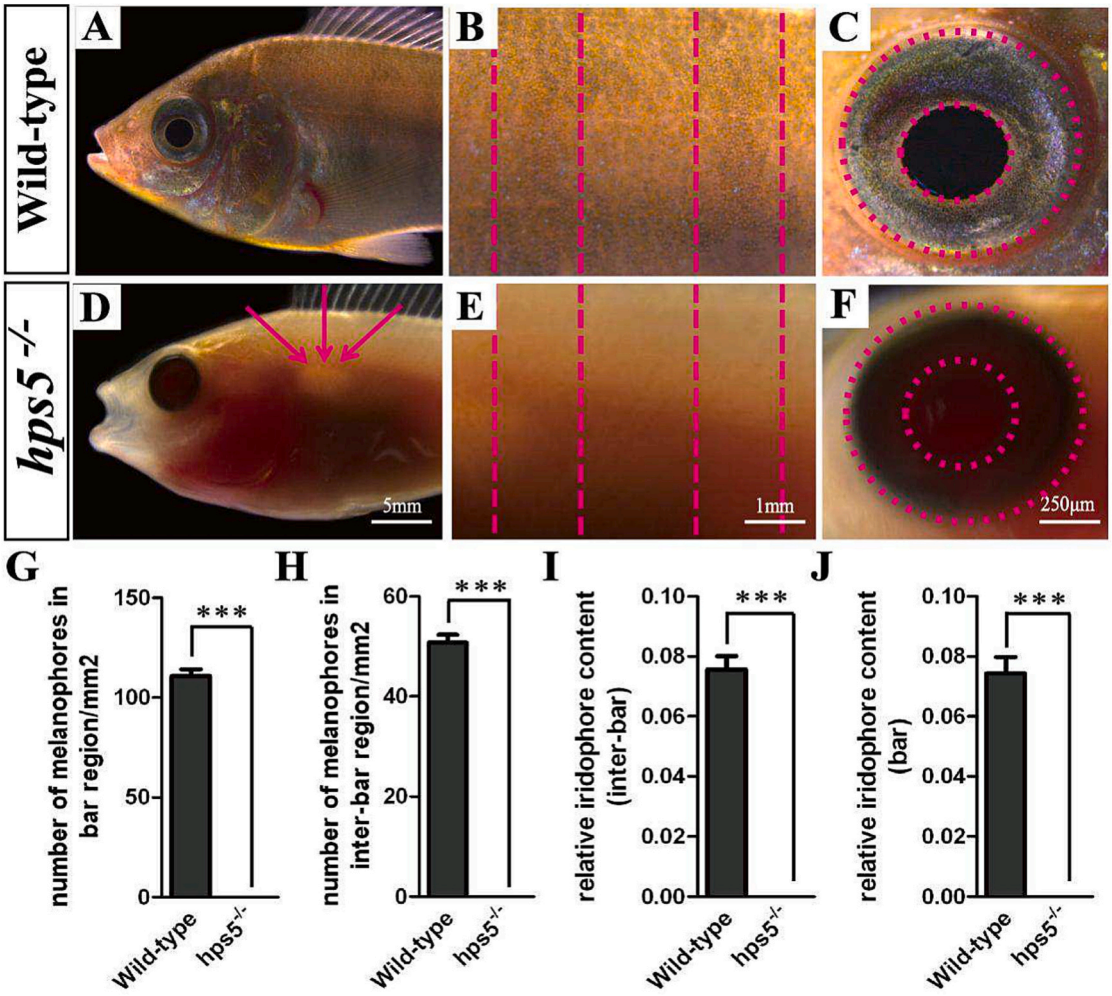

Fig. 4. Significantly decreased melanophores and iridophores were observed in the trunk and eye of the mutants at 30 dpf.
A-C: In the wild-type fish, the trunk was detected with many melanophores with higher densities in the dark bars than in the light inter-bars, and many iridophores spread in both the bars and inter-bars (A, B). The RPE was fulfilled with melanin, and the iris was detected with many iridophores and xanthophores (C). D-F: In the *hps5*$^{-/-}$ mutants, complete transparent body color with extremely inflated swimming bladder (indicated by golden arrow) was detected. No pigmented melanophores, or any iridophores were detected in the trunk and fins (D, E). No melanin was observed in the RPE which displayed dark red color, simiar to the RPE pigmentation in *hps4*$^{-/-}$ mutants. However, the iris was still in black color, with many melanosomes. The red RPE accompanied with black iris were nerver observed in any color muatants we engineered so far (F). G, H: Quantitative analysis of the numbers of the melanophores in the bar and inter-bar regions of the mutants and wild-type fish. I, J: Quantitative analysis of the relative iridophore content in the bar and inter-bar regions of the mutants and wild-type fish. Data in G-J are expressed as mean ± SD ($n = 5$). Differences in the data between the mutants and wild-type were tested by two-tailed Student's *t*-test, ***$P < 0.001$. (For interpretation of the references to color in this figure legend, the reader is referred to the web version of this article.)

both bright and transparent field (Fig. 2E).

Different from the wild-type, very few pigmented melanophores were detected on the yolk sac of the *hps5*$^{-/-}$ mutant embryos. At 3 dpf there were no melanophores and iridophores in the iris (Fig. 2F). A few hypo-pigmented melanophores were detected on the yolk sac near the heart. No melanophores and very few iridophores were detected in the iris, which was covered with an obvious blood capillary network. Additionally, no melanosomes were present in the RPE, but a large accumulation of xanthophores were detected on the head at 4 dpf (Fig. 2G and Fig. S3). Surprisingly, at 5 dpf the mutant embryos showed increasing numbers of melanophores in the iris and a hypo-pigmented RPE. Very few melanophores were detected on the yolk sac, while no melanophores were detected in the head and trunk. However, increasing numbers of xanthophores were detected in the head and trunk (Fig. 2H). At 8 dpf some hypo-pigmented melanophores were seen on the top head and yolk sac, increasing numbers of large xanthophores were found on top of the head and on the body, and increasing numbers of melanosomes were detected in the iris and RPE. The peritoneum was clearly transparent at 7 dpf, which was different with the wild-type embryos (Fig. 2I). The 8 dpf mutant embryos were similar to the 7 dpf embryos, with reduced numbers of hypo-pigmented melanophores but increased numbers of xanthophores on top of the head, still and hypo-pigmentation in eyes (both RPE and iris), under both bright and transparent field (Fig. 2J).

Quantification of the pigment cell numbers revealed significant higher numbers of yolk sac melanophores in the wild-type fish than in *hps5*$^{-/-}$ mutants at 3 dpf (Fig. 2K), significant higher relative iridophore content in the iris of the wild-type fish than in *hps5*$^{-/-}$ mutants at 7 dpf (Fig. 2L), as well as significant higher number of fully pigmented head melanophores in the wild-type fish than in *hps5*$^{-/-}$ mutants at 8 dpf (Fig. 2M).

3.4. *Melanophores were hypopigmented and significantly decreased in the head of 12 dpf mutants*

Melanophores were first detected with a global distribution in wild-type fish at 12 dpf. Generally, the wild-type fish at 12 dpf had many melanophores in the trunk and on top of the head, and the peritoneum

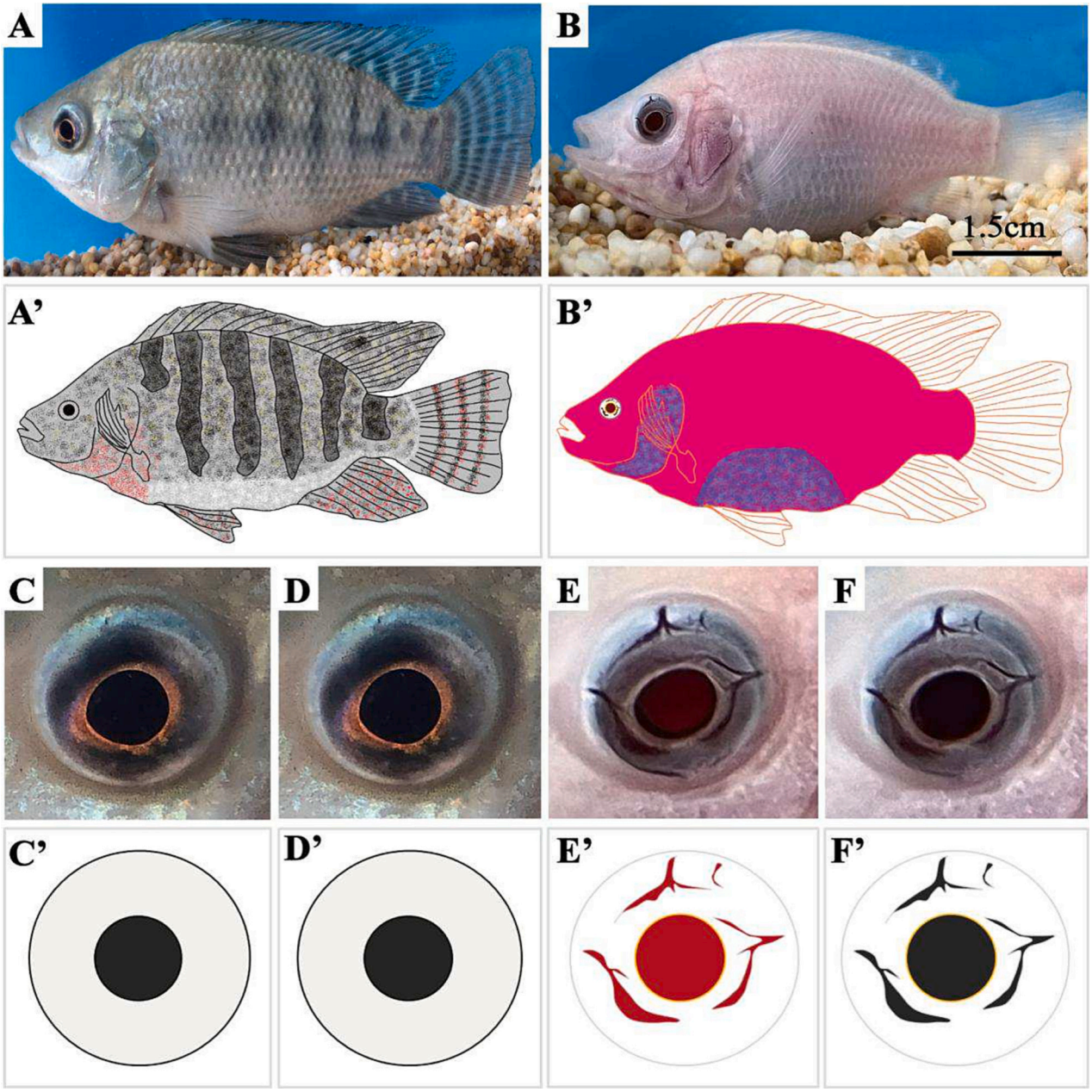

Fig. 5. No color pattern but slow restoration of guanine biosynthesis were detected in trunk and fins, and several transparent cracks were detected in iris of mutants at 90 dpf.

A, A', C, D, C′ and D′: Wild-type fish displayed hyper-pigmented vertical bars and light-colored inter-bars in trunk and fins. Both the RPE and iris were detected many mature melanosomes. The whole eyes were detected with a stable black color, no matter the eyeball moved or not, indicating plenty of mature melanosomes in the RPE. B, B′, E, F, E' and F′: The *hps5*$^{-/-}$ mutants displayed translucent body color, revealed by color of the muscle, slow restoration of white guanine development in trunk and fins and the gradual thickening of the body wall. The RPE was in dark red, but with some slow restored melanosomes. The iris displayed many white iridophores, but with several transparent cracks lacking pigmentation on it. The whole eyes were in special pigmentation. The RPE was still detected with some restored melanosomes, but not uniformly and globally spread, thus even a slight angle of eyeball movement will cause RPE to show a color change from red to black. (For interpretation of the references to color in this figure legend, the reader is referred to the web version of this article.)

was filled with iridophores and melanophores (Fig. 3A). The head and eyes (RPE and iris) both showed large numbers of mature melanosomes (Fig. 3B and C).

In contrast, the *hps5*$^{-/-}$ mutants at 12 dpf had a transparent body due to a significant loss of melanophores and complete absence of iridophores in the trunk and the peritoneum. The global body color of the mutants was yellowish-transparent. The intestines, liver and other internal organs were clearly visible, especially after their initial feeding. The "S"-shaped intestine was clearly revealed by the color of its contents. (Fig. 3D and G-3J). A magnification of the top of the head showed that the melanophores were significantly reduced in the mutants. All the remaining melanophores were hypo-pigmented, while xanthophores were significantly increased in both number and sizes (Fig. 3E and Fig. S4). Interestingly, many of the head xanthophores gathered together, indicating mutual attraction between them. Besides, the xanthophores were obviously larger in size than those in wild-type fish. Even though both the RPE and iris were hypo-pigmented, there was still lots of uniformly distributed melanin but no iridophores in the iris (Fig. 3F).

Quantification of the pigment cells revealed significant hypo-

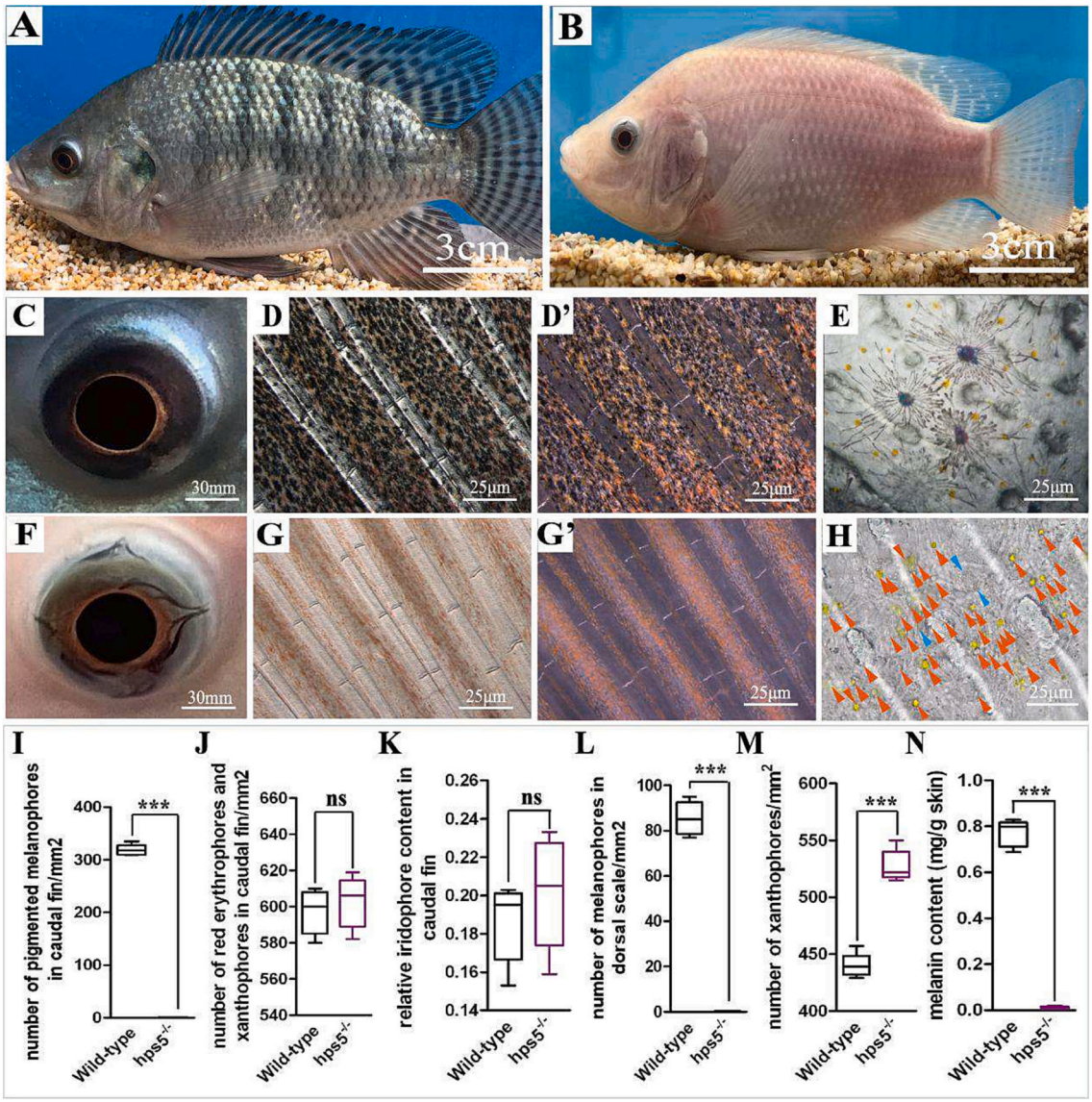

Fig. 6. Significant reduced melanophores in the trunk, iris, fins and scales, significantly increased xanthophores in scales, but no significantly increased xanthophores/erythrophores were observed in caudal fins of the mutants at 150 dpf.

A, C, D, D′ and E: The wild-type fish displayed dark bars separated by light inter-bars in the trunk and fins. The RPE was heavily pigmented, and the iris showed many melanophores. The caudal fin and scales showed many melanophores and xanthophores. B, F, G, G' and H: The *hps5*$^{-/-}$ mutants displayed black RPE and red body color with no bars in the trunk and fins due to the slow restoration of melanosome biosynthesis and enrichment of carotenoids in RPE, absence of pigmented melanophores/melanin in whole trunk and fins and slow restoration of iridophores in fins. The fins showed no pigmented melanophores but white iridophores, no significantly higher number of xanthophores and erythrophores, compared with the wild-type fish. The fins were still detected with obvious bandings and reddish pigmentation. Scales were filled with significantly increased xanthophores (yellow arrow heads) than in wild-type fish, and the xanthophores were close with each other and some of them were in a in a pigment-granule-dispersed state or even gathered together as groups. Besides, some restored white iridophores were also detected in dorsal scales (blue arrow heads). I-K: Quantitative analysis of the numbers of the pigmented melanophores, numbers of erythrophores and xanthophores and relative iridophore content in the caudal fins of the mutants and wild-type fish. L and M: Quantitative analysis of the numbers of the pigmented melanophores and xanthophores in the dorsal scales of the mutants and wild-type fish. N: Quantification of the melanin content in the dorsal skin. Abundant melanin was detected in the wild-type fish, while no melanin was detected in the mutants. Data in I-M are expressed as mean ± SD (n = 5). Differences in the data between the wild-type fish and mutants were tested by two-tailed Student's *t*-test, ***P < 0.001, ns: not significant. (For interpretation of the references to color in this figure legend, the reader is referred to the web version of this article.)

pigmentation and a smaller number of melanophores on the head and also significant lower relative melanin and iridophore contents in the iris (Fig. 3K, N and O), but significant higher relative xanthophore content and size on top head of the *hps5*$^{-/-}$ mutants than in wild-type fish at 12 dpf (Fig. 3L and M).

3.5. Significantly decreased melanophores and iridophores were observed in trunk and eye of mutants at 30 dpf

The key time point for the formation of vertical bars during metamorphosis in wild-type fish is 30 dpf, when a higher density of melanophores and larger sized melanophores appear in the bar than in the inter-bar (Fig. 4A). Many widely spread iridophores and xanthophores were detected in both the bars and inter-bars (Fig. 4B). The RPE was black with abundant mature melanosomes, while many melanophores

and iridophores were detected in the iris (Fig. 4C).

In *hps5*$^{-/-}$ mutant trunks, no pigmented melanophores or melanin were present, and no iridophores or guanine plates were observed. Hence the fish displayed a transparent phenotype. Internal organs including the gills, liver, gall and swimming bladder were still easily observed through the unpigmented skin layer and muscles (Fig. 4D). No bars or inter-bars were detected in the trunk, and xanthophores were in a pigment-dispersed state (Fig. 4E). The RPE displayed a dark red color, while the iris maintained some uniform melanosome pigmentation, along with some white iridophores (the iridophores were more easily observed when exposed under extremely strong bright field) (Fig. 4F and Fig. S5).

Consistent with the results from earlier developmental stages, quantification of the pigment cells (in both the bars and inter-bars) revealed significant fewer melanophores and iridophores in the dorsal trunk skin of *hps5*$^{-/-}$ mutants than in wild-type fish at 30 dpf (Fig. 4G-4J).

3.6. No bars in trunk but slow restoration of guanine biosynthesis in trunk, fins and eyes of mutants at 90 dpf

At 90 dpf, wild-type fish had stable black bars and inter-bars in both the trunk and the caudal fin. Their eyes, including RPE and iris, were both heavily pigmented with mature melanosomes, and thus the whole eyes had a stable black color (Fig. 5A, A', 5C, 5D, 5C' and 5D'). The wild-type fish were almost the same to the adult fish in both color patterning and shape.

In contrast at 90 dpf the *hps5*$^{-/-}$ mutants were in a red-translucent (not complete transparent) body color. The operculum was transparent, displaying the color of the gill. No melanophores or melanin was detected in the trunk, fins and eyes (iris). Some restoration of white guanine pigmentation was detected in the dorsal scales of the trunk (Fig. S6). The iris was also filled with white guanine, giving it a strong white coloration. Some crack patterns in the iris (with almost the same location to the capillary network patches at 4 dpf) were detected which did not have any pigment, but showed the color of blood and the red RPE. Consistent with the high expression level of *hps5* in eyes of wild-type fish (Fig. S1), the whole eyes (both RPE and iris) of the mutants showed an abnormal pigmentation. As the RPE still had some melanosomes, even a slight change in observation angle caused an apparent color change from red to black (Fig. 5B, B', 5E, 5F, 5E' and 5F').

3.7. No melanophores, but some restored white iridophores, and increased xanthophores and erythrophores were detected in hps5$^{-/-}$ mutants at 150 dpf

The wild-type fish had very stable vertical bars and inter-bars at 150 dpf (Fig. 6A). The RPE and the iris were black (Fig. 6C). The fins and scales were pigmented with many melanophores. Many xanthophores distributed in the gaps between the melanophores, and many iridophores gathered in spots (Fig. 6D, D' and 6E).

In contrast, the *hps5*$^{-/-}$ mutants displayed a red body color, with no pigmented melanophores but a few restored white iridophores (Fig. 6B and Fig. S7). The operculum was still transparent. The xanthophores were present in significantly larger numbers in the dorsal scales than in wild-type fish, the distances between them were significantly smaller, and there was some clustering (Fig. S8). Interestingly, even though many xanthophores/erythrophores were detected, their numbers in the caudal fins of *hps5*$^{-/-}$ mutants were not significantly greater than in wild-type fish. In addition, some restoration of white iridophores was detected in caudal fins of the mutants, which produced reddish fins with white bandings (Fig. 6G, G', 6H and Fig. S9). The RPE of the mutants was black, indicating a slow restoration of melanosome biosynthesis. The melanosome pigmentation level in trunk, fins and iris were different with that in the RPE during development of the *hps5*$^{-/-}$ mutants. The iris still displayed the same transparent cracks of the 90 dpf fish (Fig. 6F).

Quantification of the pigment cells revealed significantly lower number of melanophores in caudal fin and dorsal scales, a significant higher number of xanthophores with correspondingly shorter distances between neighboring xanthophores in dorsal scales. Xanthophore/erythrophore and iridophore numbers in caudal fin of *hps5*$^{-/-}$ mutants were not significantly higher than in wild-type fish at 150 dpf (Fig. 6I-6M and Fig. S8). Melanin content was 0.78 mg/g skin in the wild-type fish, but no melanin was detected in the mutants (Fig. 6N). The red body color was stable from 90 dpf to 150 dpf. This phenotype remained stable for the all later life stages of the tilapia *hps5*$^{-/-}$ mutants.

4. Discussion

4.1. Disruption of HPS5 led to a red body color in Nile tilapia

Mutation of melanogenesis-related genes usually also results in changes of pigment cell relative abundance and pigment cell size in tilapia. Mutants display various body colors, including albino (*tyrb*, Lu et al., 2022), golden (*pmel* duplicates, Wang et al., 2022a), silver-white (*hps4*, Wang et al., 2022b), red and yellow (*mitf* duplicates, Wang et al., 2023). In this study, we engineered an *hps5*$^{-/-}$ mutant line using CRISPR/Cas9 in Nile tilapia. The mutants displayed a red body color. A previous study suggested that *hps5* is the locus responsible for the transparent phenotype in stickleback by genetic mapping of the natural mutants and experimentally-induced mutation (Hart and Miller, 2017). Disruption of *hps5* led to significant hypopigmentation in trunk and RPE of larval *snow white* zebrafish (Daly et al., 2013). Similarly, absence of pigmented melanophores and a significant decrease in the number of iridophores was observed in the tilapia *hps5*$^{-/-}$ mutants. However, the tilapia *hps5* mutants we engineered were detected with a red body color as an absence of pigmented melanophores and reduction of iridophores in skin during development, thus the whole fish showed a merged color of the muscle and skin. While as a slow restoration of white iridophores, the red fish was still observed with some whitish coloration, against the global red background body color. In addition, the *hps5*$^{-/-}$ mutants also displayed several transparent cracks in the iris from ~90 dpf onwards. The unique body and eye (iris) color pattern might further increase the ornamental value of the mutants.

4.2. HPS5 is indispensable for melanophore development and melanosome maturation in Nile tilapia

In this study, no pigmented melanophores were detected in trunk, fins and iris of the adult *hps5*$^{-/-}$ mutants, which was similar to the situation revealed in tilapia *hps4*$^{-/-}$ mutants. While significant fewer melanophores with immature melanosomes, and significantly increased numbers of xanthophores with larger sizes were detected on the head of the young *hps5*$^{-/-}$ mutants, which was similar to the situation revealed in our previously engineered *pmela*$^{-/-}$;*pmelb*$^{-/-}$ golden mutants (Wang et al., 2022a). The existence of hypo-pigmented melanophores with immature melanosomes in early developmental stages and the complete absence of pigmented melanophores in the trunk, fins and iris at the adult stage suggested that HPS5 is indispensable for melanosome maturation and melanophore development in tilapia, even though slow restoration of melanosome biosynthesis was detected in the RPE of the adult mutants. In our previous studies, we engineered a silver-white tilapia by disrupting *hps4*, a key member of BLOC3 complex, with CRISPR/Cas9 and investigated the roles of *hps4* in directing melanosome biosynthesis and pigment cell development of tilapia. No pigmented melanophores but large accumulation of iridophores were detected in the *hps4*$^{-/-}$ mutants, which finally led to a silver-white body color in *hps4* mutants (Wang et al., 2022b). So far, a total of nine *hps* family members have been isolated in humans and mice (Wei, 2006; Sitaram and Marks, 2012). Studies in zebrafish have suggested that *hps5* and the corresponding BLOC2 complex are closely related to melanosome

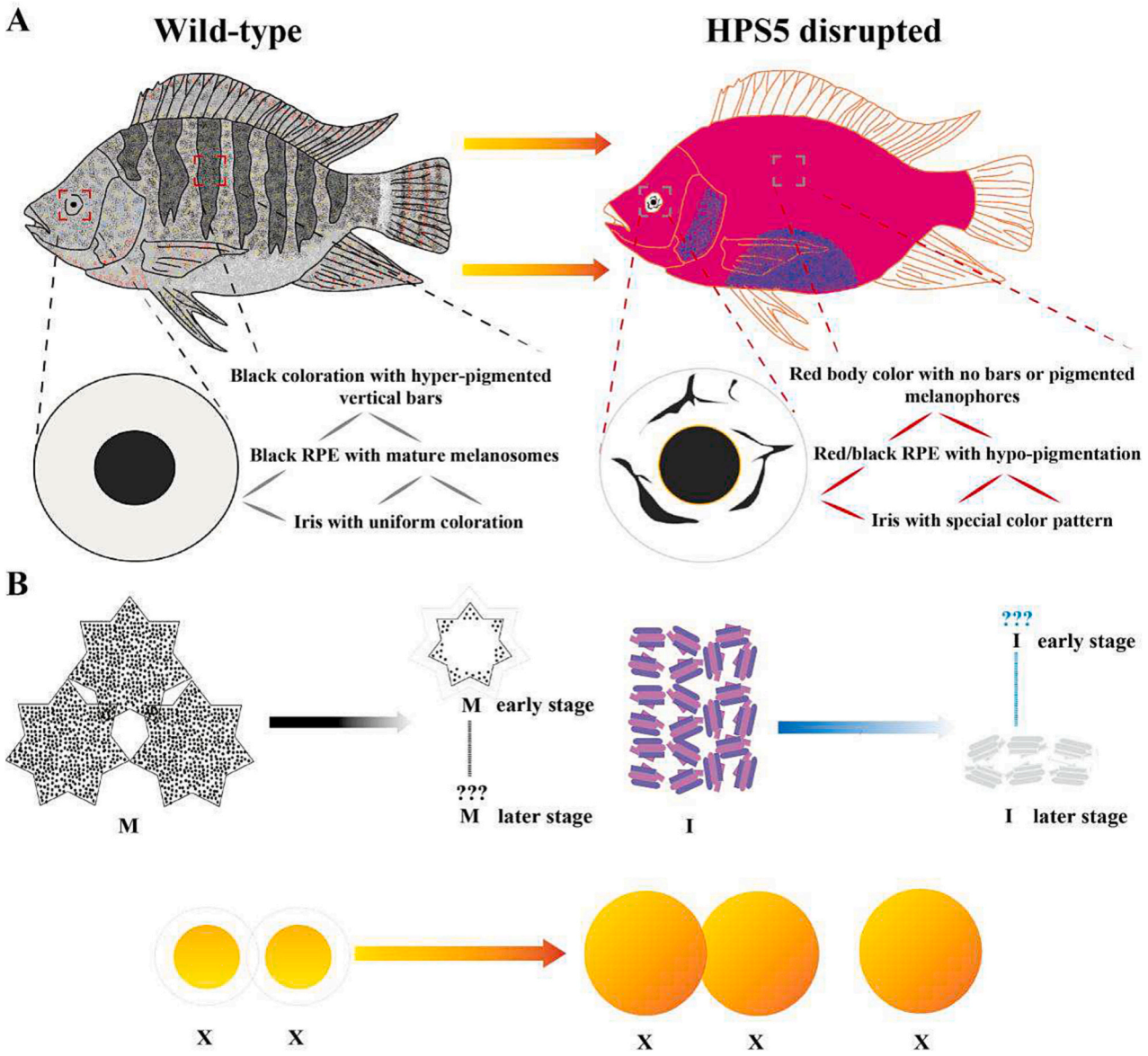

Fig. 7. Modeling on the roles of HPS5 in directing body color formation, eye color patterning and relative abundance of pigment cells of tilapia in this study. A: The wild-type fish showed stable black bars and light-colored inter-bars in the trunk and caudal fin. The eyes were detected with black RPE and the iris was also full of mature melanosomes. Black color relatively even covered the whole eyes of wild-type fish. As a contrast, the HPS5-disrupted tilapia mutants were detected with a red body color and a uniform and special eye color pattern (as the absence of melanin in whole eyes and the shortage of iridophores in the iris). No bars or inter-bars were detected in the whole mutants, as the great loss of even absence of pigmented melanophores and iridophores. B: The wild-type fish had many pigmented melanophores, however, the mutants were short of or even absent of pigmented melanophores, especially during development. The remaining melanophores in younger mutants were significantly hypo-pigmented, reflected by less number and no mature melanosomes. However, the number and sizes of xanthophores were significant increased compared with the wild-type fish, and many of the xanthophores even gathered together as groups. Distances between each of the xanthophores were less than in wild-type fish, indicating changes of the cell-cell interactions of xanthophores in the mutants. Additionally, the tilapia HPS5-disrupted mutants were also detected with significant reduction or even absence of iridophores. While due to slow restoration of iridophores during development, the whole fish showed a red body color with reddish fins as the relative abundance changes of all the major three types of pigment cells and gradual thickening of the body wall. (For interpretation of the references to color in this figure legend, the reader is referred to the web version of this article.)

development and maturation (Daly et al., 2013). In silkworm and *Drosophila*, mutation of *hps5* also results abnormal melanosome development and maturation (Fujii et al., 2012; Falcón-Pérez et al., 2007; Syrzycka et al., 2007). Besides, studies in channel catfish also suggest the similar role of *hps4* and the corresponding BLOC3 complex in directing melanosome development and maturation (Li et al., 2017). Taken together, these results indicate that the functions of BLOC super family genes, like other melanogenesis pathway genes, are probably highly conserved in melanogenesis in vertebrates and invertebrates.

4.3. HPS5 was necessary for iridophore survival and guanine biosynthesis, and fundamental for the abundance of xanthophores

The HPS5-disrupted tilapia showed a great reduction of both melanophores and iridophores, similar to the results of *hps5* mutation in zebrafish (Daly et al., 2013) and stickleback (Hart and Miller, 2017). Thus *hps5* is not only fundamental for melanosome biosynthesis and melanophore development, but also affects guanine biosynthesis and iridophore development in tilapia. Additionally, we also detected a significantly higher number of xanthophores in the head and scales of the *hps5*$^{-/-}$ mutants, and the xanthophores were also significantly

larger in the mutants than in wild-type fish. The relative abundance and sizes of xanthophores were quite similar to our previously engineered PMEL-disrupted golden tilapia mutants (Wang et al., 2022a). Importantly, the average distance between the neighboring xanthophores in the scales of the mutants were significantly shorter than that in the wild-type fish, and many of the xanthophores even gathered as groups to display stronger yellow/golden coloration (Fig. S8). These results suggested that mutual attraction among xanthophores of the mutants. Even though we did not detect a significant increase in erythrophore number in the *hps5*$^{-/-}$ mutants during development, the adult mutants still showed a red body color and reddish fins due to the significant reduction or even abscence of melanophores and iridophores, and accumulation of xanthophores. These results were different from the HPS5 mutants in stickleback, in which there did not appear to be an increase in xanthophores at 10 dpf, and the adult males had no erythrophores (Hart and Miller, 2017).

Even though a slow restoration of iridophore development was detected in the later developmental stages of the tilapia *hps5*$^{-/-}$ mutants, the iridophore survival and guanine development were still greatly limited, especially in the trunk skin and scales, and a red body color was observed. The *hps5*$^{-/-}$ tilapia mutants still had white bandings in the fins, as reported in *hps4*$^{-/-}$ tilapia mutants (Wang et al., 2022b), indicating that some unpigmented melanophores were probably still present because the bars and stripes are formed by the close cell-cell "run and chase" interactions of melanophores, xanthophores and iridophores (Watanabe et al., 2012; Yamanaka and Kondo, 2014). The tilapia *hps5* gene was not only necessary for iridophore survival and guanine biosynthesis, but also fundamental for the relative abundance of the major three types of pigment cells.

4.4. Both the RPE pigmentation and iris color pattern were affected by hps5 in Nile tilapia

By comparing the eye pigmentation of the engineered color mutants with the natural red mutants (red tilapia) and wild-type fish, we found that the eye (RPE) pigmentation and trunk color were probably controlled by different genes (Wang et al., 2021). In this study, we found that disruption of *hps5* led to a hypo-pigmented RPE at early stage and a black RPE (due to the slow restoration of melanosome biosynthesis and carotenoid enrichment) at the adult stage, similar to our previously engineered *hps4*$^{-/-}$ mutants (Wang et al., 2022b). Much to our surprise, we found the *hps5*$^{-/-}$ mutants displayed several transparent cracks in the iris from ~90 dpf onwards, due to absence of melanin, xanthophores and iridophores in specific area. Up to now, no similar phenotype in iris has been reported in any other vertebrates, the dynamic process on the formation of the transparent iris cracks needs to be better illustrated as no iris cracks were detected before 30 dpf but several permanent transparent cracks were detected at 90 dpf (as we showed in this study). In addition, further analysis on histological sections of eyes during development would be necessary for more accurately showing the phenotype differences in eyes between the wild-type fish and the mutants, and the detailed mechanisms also deserve further investigation.

5. Conclusion

In this study, we engineered a red tilapia by disrupting *hps5* in Nile tilapia with CRISPR/Cas9. The mutants displayed a red body color with reddish fins due to significant reduction or even absence of melanophores/iridophores and their corresponding pigments. In addition, the mutants displayed significant more large xanthophores, a black RPE and several transparent cracks in the iris (Fig. 7A). Developmentally, a few hypo-pigmented melanophores with immature melanosomes appeared on top of the head in early stages (5–12 dpf) in the mutants, but disappeared later. No iridophores were observed at early stages (before ~30 dpf) in the mutants, while a few iridophores with white coloration were appeared later (Fig. 7B). These results demonstrate that *hps5* is indispensable for melanophore, iridophore and even xanthophore development. To our knowledge, this is the first report on *hps5* mutation in farmed fishes. The red tilapia mutants we engineered may have potential to serve as new germplasm for aquaculture, or function as a gene resource for genetic modification and breeding of red tilapia and the other related ornamental and food fish in aquaculture.

Author contributions

DW acquired the funding, designed research, conducted investigation and administrated the project; CW created the mutants; TDK suggested strategies for phenotype analysis; CW participated in methodology application, software analysis and data collection; HL, ZW and JY participated in data collection; CW and DW curated the data and wrote the original draft; CW, TDK and DW reviewed and edited the finalized manuscript.

Supplementary data to this article can be found online at https://doi.org/10.1016/j.aquaculture.2023.740496.

CRediT authorship contribution statement

Chenxu Wang: Data curation, Formal analysis, Investigation, Resources, Software, Validation, Visualization, Writing – original draft, Writing – review & editing. **Thomas D. Kocher:** Methodology, Writing – review & editing. **Hao Liu:** Formal analysis, Validation. **Zilong Wen:** Formal analysis, Validation. **Jiawen Yao:** Formal analysis, Validation. **Deshou Wang:** Conceptualization, Data curation, Funding acquisition, Investigation, Project administration, Supervision, Writing – original draft, Writing – review & editing.

Declaration of Competing Interest

The authors declare that they have no known competing financial interests or personal relationships that could have appeared to influence the work reported in this paper.

Data availability

No data was used for the research described in the article.

Acknowledgements

This work was supported by Grant 2022YFD1201600 from the National Key Research and Development Program of China, grants 32373106, 31872556 and 31861123001 from the National Natural Science Foundation of China and grant CQFTIU2022-01 from Chongqing Fishery Technology Innovation Union. We thank Dr. Xingyong Liu and Shuqing Zheng for technical support and fish caring.

References

Bian, C., Li, R., Wen, Z., Ge, W., Shi, Q., 2021. Phylogenetic analysis of core melanin synthesis genes provides novel insights into the molecular basis of albinism in fish. Front. Genet. 12, 707228.

Braasch, I., Brunet, F., Volff, J.N., Schartl, M., 2009. Pigmentation pathway evolution after whole-genome duplication in fish. Genome. Biol. Evol. 7, 479–493.

Brawand, D., Wagner, C.E., Li, Y.I., Malinsky, M., Keller, I., Fan, S., et al., 2014. The genomic substrate for adaptive radiation in African cichlid fish. Nature 513, 375–381.

Daly, C.M., Willer, J., Gregg, R., Gross, J.M., 2013. *Snow white*, a zebrafish model of Hermansky-Pudlak syndrome type 5. Genetics 195 (2), 481–494.

Falcón-Pérez, J.M., Romero-Calderón, R., Brooks, E.S., Krantz, D.E., Dell'Angelica, E.C., 2007. The *Drosophila* pigmentation gene *pink* (*p*) encodes a homologue of human Hermansky-Pudlak syndrome 5 (HPS5). Traffic 8 (2), 154–168.

Fujii, T., Banno, Y., Abe, H., Katsuma, S., Shimada, T., 2012. A homolog of the human Hermansky-Pudluck syndrome-5 (HPS5) gene is responsible for the *oa* larval translucent mutants in the silkworm, *Bombyx mori*. Genetica 140 (10–12), 463–468.

Hart, J.C., Miller, C.T., 2017. Sequence-based mapping and genome editing reveal mutations in stickleback *hps5* cause oculocutaneous albinism and the *Casper* phenotype. Genes Genomes Genetics (Bethesda) 7 (9), 3123–3131.

Hirobe, T., Ito, S., Wakamatsu, K., 2013. The mouse *ruby-eye*^{2d} (*ru*^{2d}/*Hps5*$^{ru2\cdot d}$) allele inhibits eumelanin but not pheomelanin synthesis. Pigment Cell Melanoma Res. 26 (5), 723–726.

Li, Y., Geng, X., Bao, L., Elaswad, A., Huggins, K.W., Dunham, R., et al., 2017. A deletion in the Hermansky-Pudlak syndrome 4 (*Hps4*) gene appears to be responsible for albinism in channel catfish. Mol. Genet. Genomics 292 (3), 663–670.

Lu, B., Liang, G., Xu, M., Wang, C., Tan, D., Tao, W., et al., 2022. Production of all male amelanotic red tilapia by combining MAS-GMT and *tyrb* mutation. Aquaculture 546, 737327.

Mériot, M., Hitte, C., Rimbault, M., de Citres, C.D., Gache, V., Abitbol, M., 2020. Donskoy cats as a new model of oculocutaneous albinism with the identification of a splice-site variant in *Hermansky-Pudlak syndrome 5* gene. Pigment Cell Melanoma Res. 33 (6), 814–825.

Schneider, C.A., Rasband, W.S., Eliceiri, K.W., 2012. NIH image to ImageJ: 25 years of image analysis. Nat. Methods 9 (7), 671–675.

Sitaram, A., Marks, M.S., 2012. Mechanisms of protein delivery to melanosomes in pigment cells. Physiology (Bethesda) 27 (2), 85–99.

Sun, Y.L., Jiang, D.N., Zeng, S., Hu, C.J., Ye, K., Yang, C., et al., 2014. Screening and characterization of sex-linked DNA markers and marker-assisted selection in the Nile tilapia (*Oreochromis niloticus*). Aquaculture 433, 19–27.

Syrzycka, M., McEachern, L.A., Kinneard, J., Prabhu, K., Fitzpatrick, K., Schulze, S., et al., 2007. The *pink* gene encodes the *Drosophila* orthologue of the human Hermansky-Pudlak syndrome 5 (*HPS5*) gene. Genome 50 (6), 548–556.

Wang, C., Lu, B., Li, T., Liang, G., Xu, M., Liu, X., et al., 2021. Nile tilapia: a model for studying teleost color patterns. J. Hered. 112 (5), 469–484.

Wang, C., Xu, J., Kocher, T.D., Li, M., Wang, D., 2022a. CRISPR knockouts of *pmela* and *pmelb* engineered a golden tilapia by regulating relative pigment cell abundance. J. Hered. 113 (4), 398–413.

Wang, C., Kocher, T.D., Lu, B., Xu, J., Wang, D., 2022b. Knockout of Hermansky-Pudlak syndrome 4 (*hps4*) leads to silver-white tilapia lacking melanosomes. Aquaculture 559, 738420.

Wang, C., Kocher, T.D., Wu, J., Li, P., Liang, G., Lu, B., et al., 2023. Knockout of microphthalmia-associated transcription factor (*mitf*) confers a red and yellow tilapia with few pigmented melanophores. Aquaculture 565, 739151.

Watanabe, M., Watanabe, D., Kondo, S., 2012. Polyamine sensitivity of gap junctions is required for skin pattern formation in zebrafish. Sci. Rep. 2, 473.

Wei, M.L., 2006. Hermansky-Pudlak syndrome: a disease of protein trafficking and organelle function. Pigment Cell Res. 19 (1), 19–42.

Yamanaka, H., Kondo, S., 2014. *In vitro* analysis suggests that difference in cell movement during direct interaction can generate various pigment patterns *in vivo*. Proc. Natl. Acad. Sci. U. S. A. 111 (5), 1867–1872.